Polymer Testing 121 (2023) 107987

Contents lists available at ScienceDirect

Polymer Testing

journal homepage: www.elsevier.com/locate/polytest

Understanding the recovery behaviour and the degradative processes of EPDM during ageing

Maha Zaghdoudi *, Anja Kömmling, Matthias Jaunich, Dietmar Wolff

Bundesanstalt für Materialforschung und -prüfung (BAM), Unter den Eichen 44-46, 12203, Berlin, Germany

ARTICLE INFO

Keywords:
Compression set
Ageing
Recovery
Degradative processes
Leakage rate

ABSTRACT

Recovery is an important measure for seal applications representing to which extent the elastomer regains its initial shape after deformation and release of an applied force. Compression set (CS) indicates the degree of recovery. Ethylene propylene diene rubber (EPDM) was aged at 75 °C, 100 °C, 125 °C and 150 °C for different ageing times up to five years and compression set measurements were performed at different times after disassembly and after additional tempering. Short- and long-term recovery up to one year after release for samples aged at 125 °C and 150 °C was also studied. To assess the curvature in the Arrhenius diagram that may occur due to non-sufficiently aged specimens, a degradation-rate based model was fitted to the CS data after tempering. For each ageing temperature, two decay fit functions were proposed, each with an activation energy and a corresponding degradative process. The influence of ageing on the leak-tightness after fast small partial release is investigated and estimated through the analysis of the shift factors from time temperature superposition (TTS) of CS measurements at different times after disassembly. Shift factors of CS measurement after 1 s and after additional tempering are in good agreement.

1. Introduction

Elastomers are often used in sealing applications due to their high resilience. However, depending on the field of application, the seal can be exposed to harsh environment, temperature and static or dynamic mechanical loading. The combination of temperature and mechanical loading in air is probably one of the most encountered environmental influences in application and results in thermo-oxidative ageing of the rubber component [1]. Thermo-oxidative ageing strongly affects the mechanical behaviour of rubber products and limits their lifetime [2]. To understand the long-term thermal and thermo-mechanical degradation of elastomeric components and to predict their lifetime under operating conditions, one possible approach is to perform accelerated ageing experiments. Accelerated ageing aims at reproducing the effect of ageing at operating conditions in a shorter time by raising e.g. the test temperature [3]. The change of physical properties or chemical alterations caused by accelerated thermo-oxidative ageing is then extrapolated to the temperature of interest. However, before starting the extrapolation of ageing data, accelerated ageing experiments must be first planned over an appropriate time/temperature range. For this, degradation mechanisms and possible ageing-related heterogeneities such as diffusion-limited oxidation (DLO) [4] that might occur only during accelerated ageing and not under operating conditions must be understood to effectively prevent their occurrence during the tests. For that, the samples must be analysed with regard to inhomogeneous effects after the tests to ensure reliability of the produced data.

In sealing applications, compression set (CS) represents the recovery behaviour of a seal after ageing in compression and is one of the key indicators of the seal's long-term performance. CS is influenced by the viscoelastic behaviour of the material [5] as well as chain scission and crosslinking reactions which occur e.g. when the seal undergoes thermo-oxidative ageing during operation [6]. As CS is a time-dependent property, measuring CS at different times after release from compression yields different results with corresponding information about the material's recovery behaviour at the respective time scales. Therefore, CS was measured at different times after release in this study: during the first hour, after 30 min (as specified in standards ASTM D395 and DIN ISO 815-1 [7,8]) and at several times up to one year (abbr. a) and after additional tempering to reach equilibrium. Understanding the recovery behaviour and the degradation that results from thermo-oxidative ageing is required to make reliable lifetime predictions for safe operation (e.g., for transport and storage of nuclear waste

* Corresponding author.
E-mail address: Maha.zaghdoudi@bam.de (M. Zaghdoudi).

https://doi.org/10.1016/j.polymertesting.2023.107987
Received 3 January 2023; Received in revised form 17 February 2023; Accepted 9 March 2023
Available online 10 March 2023

containers) [9]. To assess the presence of a curvature in Arrhenius plots due to insufficiently aged samples, a degradation rate based model [10] was applied to the CS data after tempering. Different degradative processes that are predominant either in the early or later stages of ageing are identified and discussed. Generally, a static seal is considered to have reached the end of its service life when the leakage rate of the system exceeds a specified threshold value. However, even under purely static conditions, a safety margin for small dynamic events should be considered for lifetime predictions. This was implemented by including a modified leakage test with a small fast partial release of the seal during the pressure rise measurement (from ~25% to ~23% compression in less than 1 s) [11,12]. A seal becomes untight when it is not able to follow the releasing flange after quick partial release. A gap between the flange and the seal representing a leakage path forms and the seal is not tight anymore. If the seal recovers sufficiently, the formed gap can be closed again over time but nevertheless even the temporarily present gap can lead to unacceptable leakage. To link the seal tightness to the seal resilience, one possible solution is to analyse the recovery behaviour at different time scales and correlate it to leakage tests. For example, the recovery measured directly after release from compression correlates much better to the seal situation in the leakage test with partial decompression than the value measured after 30 min according to the standards.

To assess the influence of ageing on the leak-tightness during dynamic fast partial release, the shift factors from time temperature superposition (TTS) of CS data with different measurement times after release and after additional tempering are analysed and compared to those from leak-tightness tests.

2. Material and methods

Ethylene propylene diene rubber (EPDM) O-rings with a cord diameter of 10 mm and an inner diameter of 190 mm were studied. The material contains 48 wt% ethylene, 4.1 wt% ethylidene norbornene (ENB), 90 phr carbon black fillers and no plasticiser and is the same as used in previous studies [4,6,10–12]. All tests were performed on O-ring material. O-ring segments with 1 cm length were utilised for the compression set measurements with the dynamic mechanical analysis (DMA) device. For compression set measurements according to the DIN ISO 815-1 [8] and at different times after disassembly, two half O-rings were aged compressed and both were used for the applied measurement approach. As for the compression set measurements after additional tempering for 1 day (abbr. d), one of the half O-rings was used. For the leakage rate measurements, full O-rings were employed. In the following the applied methods, such as different approaches on compression set and leakage rate measurements, are described.

The abbreviation of time units used in the following sections are shown in Table 1.

2.1. Compression set (CS)

2.1.1. CS measured with DMA device

Measurements were conducted on a Gabo Eplexor 500 N (Netzsch Gabo, Germany) device. O-ring segments of 10 mm length were used as samples and were radially compressed by 25% at room temperature (RT). The O-ring segments were left compressed by 25% while heated to the test temperature with a heating rate of 1 K/min. After that the samples were kept compressed at test temperature (TT) for a defined ageing time as shown in the DMA temperature deformation program in Fig. 1. During ageing in compressed state, the compression force which decreased because of relaxation was measured. At the end of the defined ageing time, the compressed O-ring segments were cooled down to RT with a cooling rate of 1 K/min. Afterwards, the force was rapidly decreased within 20 s to a low contact force of 0.5–1 N, which is required to perform the subsequent recovery measurements for 60 min. The latter has only a minimal influence on the delivered values. The sample height was measured with a time increment of 1 s for the first 10 min after release (600 measurement points). For the remaining time (50 min), 340 measurement points were taken with a time increment of 10 s. The value of CS at t = 0 which corresponds to the first delivered value from the DMA device after reducing the compression force to the contact force is called CS_0.

Table 1
List of time unit symbols.

Second(s)	s
Minute(s)	min
Hour(s)	h
Day(s)	d
Year(s)	a

2.1.2. CS measurement according to DIN ISO 815-1 at different times after decompression

In contrast to the standards, CS was measured on O-ring segments (Fig. 2(b)) instead of standard cylindrical samples (Fig. 2(a)). Half O-rings were aged in compressed state between metal plates. The plates with the half O-rings were taken from the ageing oven at a given ageing time and left compressed during cooling to room temperature before the plates were disassembled.

According to standards ASTM D395 and DIN ISO 815-1 [7,8], the recovered height h_2 is measured after 30 ± 3 min. CS is calculated from Eq. (1) where h_0, h_1 and h_2 are the initial, the compressed and the recovered height of the sample, respectively.

$$CS(\%) = \frac{h_0 - h_2}{h_0 - h_1} \cdot 100\% \quad (1)$$

Ten positions on each half O-ring were measured and the average values were used. When CS = 0% (i.e. $h_2 = h_0$), the sample shows a complete elastic recovery. For CS = 100% (i.e. $h_2 = h_1$), the sample presents no recovery. Additionally, for samples aged at 125 °C and 150 °C, h_2 was measured at different times after disassembly for up to 1 a.

2.1.3. CS measured after tempering

To accelerate the recovery towards equilibrium [14], half O-rings that were already aged in compressed state at 75 °C, 100 °C, 125 °C and

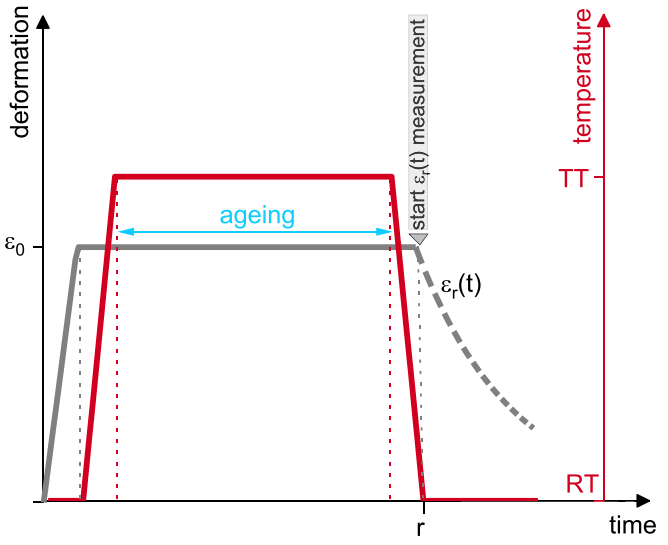

Fig. 1. Schematic representation of the temperature-deformation program of the DMA.

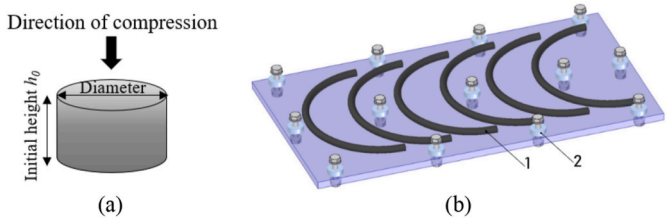

Fig. 2. Schematic representation of the configuration for determining the compression set according to (a) DIN ISO 815-1 with cylindrical samples [8] and (b) used test setup with six half O-rings of three different materials [13] (1 - Specimen and 2 - Spacer).

150 °C were disassembled at RT and later placed in an oven for 1 d at 100 °C. The recovered height after this thermal conditioning was measured at RT and used for calculating the CS after tempering.

2.2. Leakage rate

The leakage rate measurements were carried out with the pressure rise method. During the pressure rise measurements a small rapid partial decompression from 25% to 23% compression in less than 1 s was performed with a homemade apparatus [11,12,15]. Each measurement lasted 2 h and the leakage rate (Q) is calculated from the pressure difference (Δp), the volume V inside the compressed O-ring between the flanges as well as the connecting pipes to pressure gauge and vacuum pump, and the time interval Δt by means of the following equation:

$$Q(t) = \frac{\Delta p(t).V}{\Delta t} \cdot 100\% \quad (2)$$

3. Results and discussion

3.1. Physical recovery

The physical recovery is investigated through the analysis of CS results at different times after load removal. On the time scale, the recovery is assessed by short- and long-term measurements after load removal. The short-term includes measurements taken up to 1 h after release while the long-term extends up to 1 a after disassembly.

3.1.1. Short-term physical recovery

In general, the CS measurements were conducted according to the standards (except for the differing sample geometry). However, regarding the function of a seal under e.g. accident scenarios with short decompression times, the short-term recovery after release presents a key information. Fig. 3(a) and (b) represent the evolution of CS of samples aged for 1 d, 3 d and 10 d at 125 °C and 150 °C measured with the DMA device as well as the results according to DIN ISO 815-1 [8] standard measured after 30 min. As explained in section 2, the heating or ageing in air was performed in the heating chamber of the DMA device for the CS measured with the DMA. As for CS measured according to DIN ISO 815-1, the ageing was done in an air circulating oven. As it can be seen for the results delivered with the DMA device, a strong decrease of CS is recorded at the early stages after release until approximately 10–15 min. This strong decrease is followed by a linear gradual drop which could be approached by an asymptote. Some quantitative differences exist between the results taken with the DMA device and those obtained according to DIN ISO 815-1. Such a deviation between the measurement results may be due to an uncertainty on the time scale of the samples measured according to the standard, as the disassembly of the 13 screws that fixed each of the plate pairs and the measurements each took several minutes. Additionally, some samples stuck to the plates and were hard to detach. Meanwhile, the samples continued to recover, which could account for the lower values of the standard measurements compared to the continuous results.

For a deeper analysis of the time dependency of the recovery, it was attempted to fit the experimental results shown in Fig. 3 with different exponential decay functions. However, the obtained fits presented a poor correlation to the experimental data. Therefore, the CS from the DMA was normalised to CS_0 which corresponds to the first delivered recovery value from the DMA device after release of the compression force. The ratio CS/CS_0 represents the normalised recovery in % after release to allow fitting of the data. Fig. 4 shows the evolution of the ratio CS/CS_0 of EPDM for the investigated ageing temperatures (125 °C and 150 °C) and times (1 d, 3 d and 10 d). Here a total of 940 datapoints were taken by the DMA within 60 min after load removal with different time increments as explained in the method section. For the sake of clarity of the plots only one out of 10 measurement points is presented for the first 12 min and afterwards every 20th point.

The curves display an exponential decay over time. For the fit functions presented in Fig. 4, three retardation times with $\tau_1 = 0.3$ min, $\tau_2 = 3$ min and $\tau_3 = 30$ min are chosen. The correlation coefficients presented in Table 2 show a good agreement with the chosen third order exponential decay function (Eq. (3)), where A_i stands for retardation strengths, τ_i for retardation times and Y_0 for a constant value of the ratio CS/CS_0 that is reached after "infinite" time.

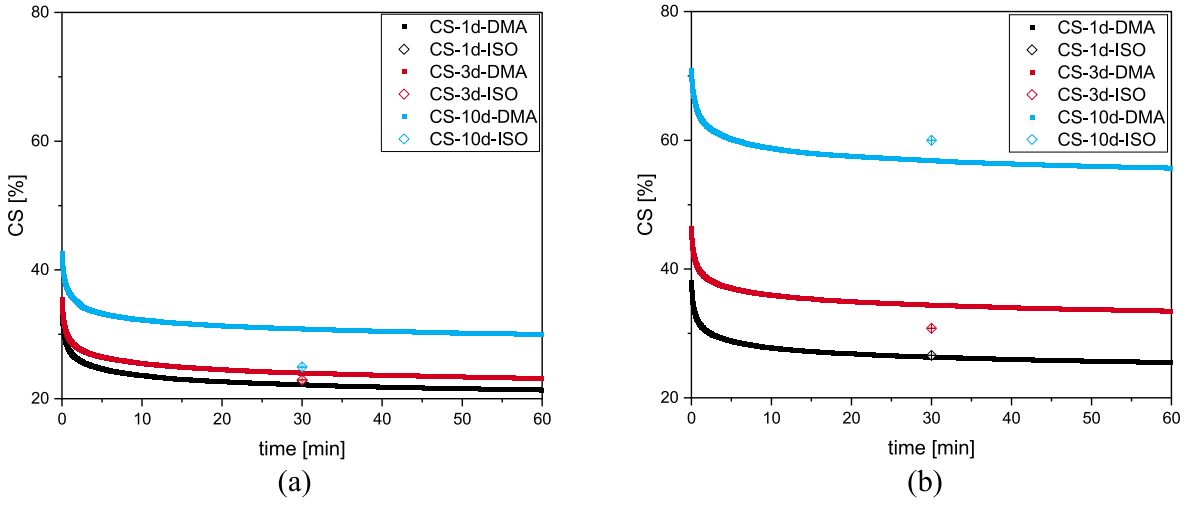

Fig. 3. Evolution of CS over time and the CS results measured according to DIN ISO 815-1 for EPDM aged at (a) 125 °C and (b)150 °C for 1 d,3 d and 10 d. The data points for CS-ISO for 1 d and 3 d at 125 °C overlap.

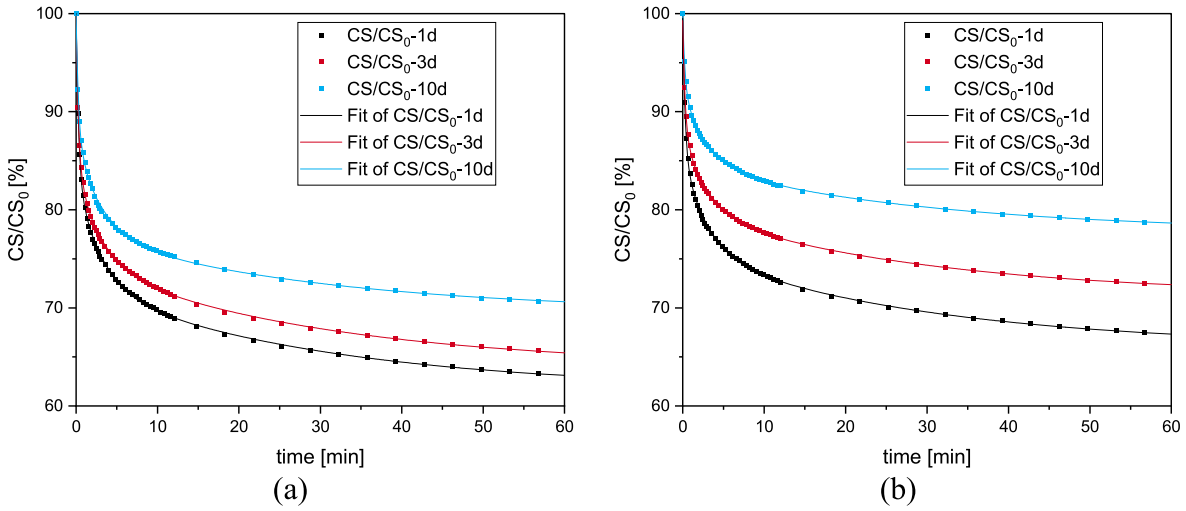

Fig. 4. Evolution of the recovery in % after release in terms of CS/CS_0 with their fit functions for EPDM aged at (a) 125 °C and (b)150 °C.

Table 2
Y_0 fit parameter and correlation coefficients of the fit functions in Fig. 4.

	Y_0 [%]			R^2		
	1 d	3 d	10 d	1 d	3 d	10 d
125 °C	61.7	64	69.6	0.999	0.999	0.998
150 °C	66	71.2	77.8	0.999	0.999	0.999

$$\frac{CS}{CS_0} = Y_0 + \sum_{i=1}^{3} A_i e^{-\frac{t}{\tau_i}} \tag{3}$$

The ratio CS/CS_0 in Fig. 4 represents the recovery up to 1 h after disassembly. Full elastic recovery with a value equal to zero would theoretically be reached as time tends to infinity according to Eq. (3) when $Y_0 = 0\%$. However, depending on the degree of degradation (ageing temperature and extended ageing times), complete recovery will not occur and an "irreversible" set which increases with the degree of degradation is expected as presented in Table 2. Larger values mean higher degree of degradation/higher set. The value of Y_0 would be slightly affected by changing the order of the fit function in Eq. (3). A change in Y_0 would also be expected when the time frame of the conducted experiment is noticeably longer than 1 h. This implies that Eq. (3) is only applicable in the temporary measurement domain corresponding to 1 h after disassembly to analyse the short-term physical recovery.

For further understanding of the recovery process, the dependency of the retardation strengths to ageing time is shown in Fig. 5. Generally, the A_i decrease with ageing time, implying less recovery. An exception is shown for samples aged at 125 °C regarding A_2. It was expected that A_2, which is related to the intermediate relaxation time $\tau_2 = 3$ min, decreases with ageing time. However, when comparing the A_2 values of samples aged at 125 °C for 3 d and 10 d, the value of the latter is higher than that of the other one. No general conclusion could be drawn regarding the retardation strength of the intermediate relaxation times. On the other hand, the parameter A_1 presents the strongest ageing time dependency. According to the measurement data presented in Figs. 3 and 4, the sample exhibits a very strong recovery shortly after release. Since the retardation times were set, the parameter A_1 related to the shortest retardation time $\tau_1 = 0.3$ min describes this fast recovery. For both parameters A_2 and A_3 smaller ageing dependency compared to A_1 are observed within the given time domain (60 min after release). When comparing the A_i values in Fig. 5(a) and (b), it is shown that the higher the ageing temperature, the smaller the A_i. The same ascertainment is found for the ageing times. This indicates that the recovery is slower for higher degradation states (i.e. the couple of variables ageing

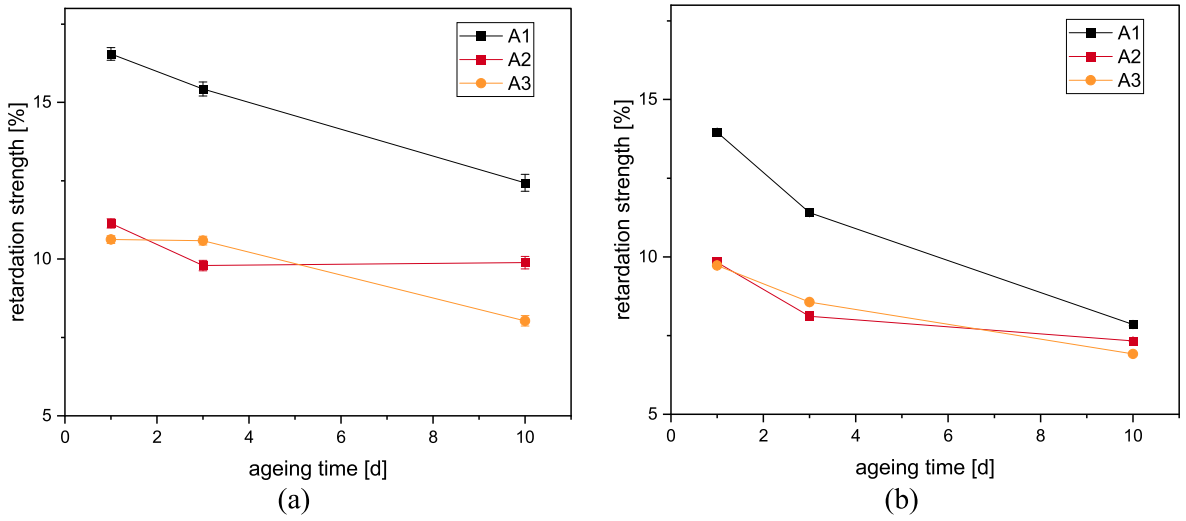

Fig. 5. Relative retardation strength over ageing time for (a)125 °C and (b)150 °C. The error bars represent the standard errors of the fit. In (b) error bars are within the symbols.

temperature and ageing time). Note that the CS_0 values represent the first delivered data from the DMA which in terms influences mainly the A_1 values. Due to the same procedure adopted for all measurements, a relative interpretation of the results is possible.

However, the recovery proceeds longer than 60 min i.e. time of the conducted short-term recovery experiment and the long-term physical recovery will be studied in the next subsection.

3.1.2. Long-term physical recovery

Fig. 6 shows the evolution of the recovery over time of EPDM samples aged at 125 °C and 150 °C for 10 d. The measurements of CS were conducted at different times after disassembly ranging from 0.5 d to 365 d and after additional tempering. The data shows that the recovery proceeds for a long time, especially for the samples aged at 125 °C for up to 1 a. On the other hand, the recovery of the sample aged for 10 d at 150 °C did not reach the value of the tempered sample and seems to come to a halt after about 50 d. An explanation could be that the thermal energy induced by the tempering step probably enables the polymer chains to reach a further recovery state. Additionally, the difference between tempered CS and long-term CS might be due to the cold set [16] that is more pronounced the higher the ageing temperature is. As the material cools to RT, the energy and mobility of the chains is reduced so that the stress induced at higher temperature may be unable to relax at lower temperature. Additionally, the thermal expansion coefficients of the elastomer and the steel plates used for its compression are different. This induces different compressive thermal stresses upon cooling to RT.

In Fig. 6(a) fit function (Eq. (4)) is proposed, where CS_∞ is the equilibrium compression set value.

$$CS(t) = CS_\infty + A_{d1}e^{-\frac{t}{\tau_{d1}}} + A_{d2}e^{-\frac{t}{\tau_{d2}}} \quad (4)$$

The term $A_{di}e^{-\frac{t}{\tau_{di}}}$ accounts for reversible physical processes. A_{di} and τ_{di} are respectively the retardation strengths and the retardation times of the total physical recovery at a given ageing time d. For EPDM aged for 10 d at 125 °C, it has been found that a first order decay presented a good fit to the experimental results [17]. At this ageing condition, CS_∞ corresponds to the value of the CS after tempering. However, for the more degraded samples in Fig. 6(b), the first order decay function did not provide a good fit as a strong decrease of 42% CS is recorded for the first 20 d after disassembly, so that a second decay fit function (Eq. (4)) with two retardation times τ_{d1} and τ_{d2} was adopted for the EPDM aged at 125 °C and 150 °C. The fit parameters of Fig. 6 are summarised in Table 3.

It was expected that the more the sample degrades through chain scission and newly formed crosslinks, the longer the time required for recovery as it was found in the short-term physical recovery section with fixed retardation times and higher retardation strengths for the less aged samples. This was not the case for intermediate and long recovery times, as can be seen from Fig. 6 and Table 3. For the more degraded stage, the retardation times are smaller, and the retardation strength are higher as presented in Table 3. While the more aged samples (10 d at 150 °C) show less and slower recovery at the short-term scale (cf. Figs. 3 and 4), Fig. 6 shows that this is not compensated by more recovery in the long-term, but that the recovery basically stops after about 50 d, while it proceeds for about 1 a for the less aged sample (10 d at 125 °C). However, the more degraded samples exhibit higher recovery in the mid-term scale (the first 20 d after disassembly) compared to the less aged samples as it can be seen from the retardation strengths and retardation times presented in Table 3. Therefore, the better recovery of less-aged samples is due to both a faster recovery in the beginning (during the 1st h after load removal cf. Figs. 3 and 4), and more recovery in the long run. This can be explained as follows: With increasing degradation, crosslinking becomes the dominant degradation mechanism in EPDM [18]. With increasing degree of crosslinking, the mobility of the molecular chains decreases which results in a decrease of the time-dependent viscoelastic part of the recovery. This was investigated through rheological characterisation of EPDM during ageing [19]. It has been found that with increasing the ageing time and temperature, a decrease of tan δ is observed which indicates the restriction of molecular mobility until a gelation state that represents a critical extent of recombination or crosslinking reactions through thermal ageing [19]. Through the formation of new crosslinks, some of the polymer chains might be trapped in the network [20] and might not contribute to the recovery. Also, when both ends of a chain are connected in the same crosslink junction, an elastically ineffective loop will be formed [20] and the chain will not contribute to the recovery. Therefore, for the more aged samples most of the possible recovery is finished within a shorter time frame. Moreover, the difference between the CS after tempering and CS after 1 a (cf. Fig. 6(b)) might be due to the restricted mobility of the trapped chains. This restriction will be reduced if there is an external stimulator/catalyst (e.g. temperature) which improves the mobility of the chains. Additionally, it has been found that chain scission dominates in the beginning of EPDM degradation [6] which can lead to longer

Table 3
Fit parameters of Fig. 6.

	A_{d1}[%]	τ_{d1} [d]	A_{d2}[%]	τ_{d2} [d]	CS_∞ [%]	R^2
125 °C	2.06	0.41	10	29.34	9.46	0.99
150 °C	16.75	0.09	11.08	12.13	29	0.99

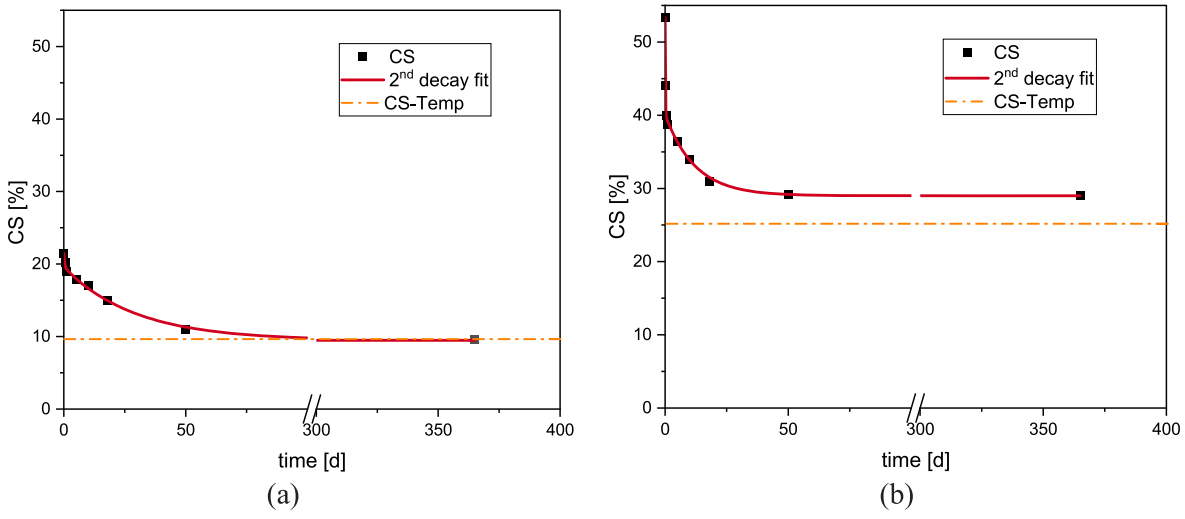

Fig. 6. Evolution of CS over time of EPDM aged for 10 d and its corresponding fit at (a) 125 °C and (b) 150 °C.

dangling chain ends and thus to a more pronounced long-term viscoelastic recovery. For EPDM aged at 125 °C for 10 d, it has been shown that crosslinking and chain scission evolve with the same macroscopic impact. For longer ageing times, chain scission still competes with crosslinking. On the other hand, the viscoelastic contribution was also investigated through the analysis of the force measured with intermittent stress relaxation [6]. It has been found that the viscoelastic contribution at 125 °C up to 185 d, which correlates with chain scission [6], increases gradually up to ~1.8 times the initial value. Thus, the chain scission effects seem to continue to dominate for longer times. For EPDM aged at 125 °C for 10 d, the viscoelastic contribution and the chain scission effects enhance the long-term recovery. At this ageing state, CS after 1 a corresponds to CS after tempering. The influence of different degradation mechanisms will also be elaborated in the next section.

CS after tempering experiment has proven its efficiency and represents a time saving procedure to determine the equilibrium CS values. Note that previously two representative samples were tempered again [13] in order to confirm that the CS after tempering corresponds to the equilibrium value. A maximum of 2% CS difference after the second tempering was found, which is acceptable and is within the error range of our CS measurement on an O-ring with approx. ± 3%.

3.2. Degradation mechanisms

The analysis of the degradation mechanisms will be carried out on the basis of CS measurements after tempering as they reflect only the irreversible chemical reactions [21] (chain scission and crosslinking). As the degradation increases with the ageing state (ageing temperature and ageing time), it is important to determine the ageing time required to assess the degradation mechanisms in the studied temperature range. In addition, samples that aged non-homogeneously should be excluded from the analysis. In our recent study of CS analysis after tempering of EPDM aged at 75 °C, 100 °C, 125 °C and 150 °C for 5 a [13], it has been shown that the shift factors for different ageing time data bases are not the same. The shift factors were examined after 0.5 a (183 d), 2 a and 5 a. Using an end-of-lifetime criterion of 70% CS [13], a good agreement between the value determined from the master curve and the measured lifetime was reached only with the shift factor of the 5 a data. When using the data after 0.5 a and 2 a, the lifetime to reach the 70% CS criterion was underestimated by 31% and 22%, respectively. Thus, the 5 a CS after tempering data will be used in the following.

In this section, a manually performed time-temperature superposition (TTS) is employed for better modelling of fit curves for the 5 a CS ageing data at 75 °C, 100 °C, 125 °C and 150 °C. For constructing the master curves, the shift factors published in Ref. [13] are used and listed in Table 4. The evolution of the CS results and the corresponding fits are shown in Fig. 7, where the grey symbols show shifted data measured at a different temperature and the coloured ones are the original data set. It is to mention that all considered experimental values are for DLO free samples [4,13]. This means samples with detected DLO effects were excluded from the shift (e.g. EPDM aged for 100 d at 150 °C). DLO occurs when the oxygen in the sample interior is consumed faster than it can be resupplied by diffusion from the surrounding atmosphere. This results in the formation of an oxidation gradient in the sample with more oxidised layers at the sample surface in comparison to the interior [22].

Table 4
Shift factors to the ageing temperatures 75 °C, 100 °C, 125 °C and 150 °C [13].

		Shift factors a_T to the ageing temperature			
		75 °C	100 °C	125 °C	150 °C
Ageing temperature	**75 °C**	1	10	90	450
	100 °C	1/10	1	9	45
	125 °C	1/90	1/9	1	5
	150 °C	1/450	1/45	1/5	1

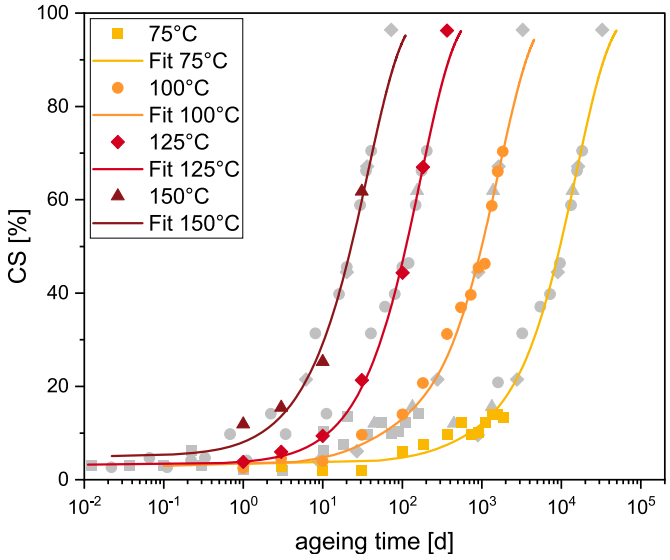

Fig. 7. Evolution of the compression set after tempering as a function of ageing time: coloured symbols showing experimental data measured at the respective temperature, grey symbols showing shifted data measured at different temperatures, solid lines showing the calculated fit function.

This could be experimentally investigated for example through microhardness [4] or indenter modulus measurements [11,23] across the section of the sample. For the fit curves, second order increasing exponential functions are chosen where B_i are the retardation strengths and t_i are the retardation times. The fit parameters and the correlation coefficients are presented in Table 5.

In the previous investigation, the different shift factors for shorter ageing times (0.5 a and 2 a) are possibly due to different degradation mechanisms that could happen at the early degradation stages [13]. Moreover, the uncertainty in the shift process could be associated with the small change of CS values at short ageing times for lower temperatures. On the other hand, for higher temperatures when the change in the property is very fast and cannot be properly captured during short ageing times, uncertainty in the shifting may occur. This is clearly emphasised in Fig. 7 for EPDM aged at 75 °C and 150 °C. It can be said that without the shifted values of the other temperatures, very different fit functions than those of Fig. 7 and Table 5 are to be expected. This is due to the low change of the property even after 5 a for the EPDM aged at 75 °C as shown in Fig. 7. On the other hand, the fast change in the property at shorter ageing times for the samples aged at 150 °C is also clearly displayed in Fig. 7 despite a small shift in the fit between 10^{-2} and 1 d due to the higher weighting of the experimental data of the test temperature. For all data, the shifted values have all together a weighting factor of 0.5 and the data measured at the respective temperature have all together the same weighting factor (i.e. 0.5). This allows the real measured data at the test temperature to have a higher impact on the fit function.

Through examining the shift factors of CS after tempering of EPDM at 75 °C and 100 °C based on the available data after 183 d and 2 a, two different slopes in the Arrhenius diagram had been found [13]. While the high-temperature range (125 °C and 150 °C) exhibited a relatively constant E_a of 90 kJ/mol and 93 kJ/mol, respectively, the

Table 5
Fit parameters used in Fig. 7.

Temperature [°C]	B_1	B_2	t_1 [d]	t_2 [d]	R^2
75	2.8	93.8	341	15328.2	0.99
100	5	92	36	1634.8	0.99
125	0.7	96.1	12.1	170.6	0.99
150	2.5	92.6	3.4	37.1	0.99

low-temperature range (75 °C and 100 °C) yielded an E_a of 58 kJ/mol after 183 d and of E_a = 71 kJ/mol after 2 a. This means that the degradation mechanisms activated in the earlier part of degradation are not the same as those after 2 a or after 5 a of degradation (or those at the higher ageing temperatures). As the Arrhenius equation cannot resolve competing processes, it cannot be said with confidence that the temperature dependency of the rate constants is consistent with a single activation energy mechanism. The assumption of different degradation mechanisms implies that at lower temperatures even for ageing until 2 a, only one degradation mechanism is dominant. On the other hand, at higher ageing temperatures this degradation mechanism cannot be easily detected since it takes place at short ageing times. This can be also seen from Fig. 7 where after ageing at 75 °C for 2.5 a, CS ≈ 12%. The same CS value is also achieved for the samples aged at 150 °C after 1 d.

However, when looking at studies in literature, low and high activation energies related to low and high temperature ranges were found through examining the CS values of Butyl Rubber. These results should be taken with caution [24]. Indeed, the performed analysis was based on CS measurements according to the DIN ISO 815-1 standard [8] (i.e., 30 min after disassembly). This measurement reflects the reversible and irreversible processes as the recovery proceeds further. Moreover, the analysis was made on samples aged up to 20 d and for CS values that do not exceed 50%. Albeit several polymers exhibit non-Arrhenius behavior [25,26], it is necessary to recall that our analysis is valid for the studied material compound and temperature range.

It has been established in our recent publication [10] conducted on the same material of the present study that two degradation mechanisms during chemical stress relaxation were involved. The first degradation mechanism is activated at shorter ageing times and loses importance at longer ageing times and/or higher ageing temperatures. The second one is only activated at longer ageing times and/or higher ageing temperatures. Each degradation mechanism has an activation energy, and the total apparent activation energy evolves as a function of the degree of degradation until reaching a saturation or a plateau. The contribution of each degradation mechanism to the overall system was subsequently established through the development of a degradation rate-based model.

The same procedure used in Ref. [10] for compression stress relaxation is adopted for CS after tempering. By plotting the inverse of the retardation times of the CS fit functions given in Table 5 in an Arrhenius diagram, linear relationships are obtained in Fig. 8.

The corresponding activation energies of 73 kJ/mol and 99 kJ/mol that correlate to the temperature dependency of the respective degradation processes are also shown in Fig. 8. Similarly to Ref. [10], the total activation energy could be connected to the single-process energies $E_a^{t_1}$ = 73 kJ/mol and $E_a^{t_2}$ = 99 kJ/mol through a simple rule of mixture that represent the fraction of processes α_i. The E_a of 73 kJ/mol for the low degradative state corresponds well to the 71 kJ/mol found for the shift of CS data after 2 a. The 58 kJ/mol obtained after 183 d deviate notably, possibly because of a large error in the shift due to the very low changes of CS at 100 °C and 75 °C at this early ageing time. To represent a progressive transition between the two states, namely the low and high degradative processes, the evolution of the fraction of process α_i is described as follows, where x is the crossover point between the α_i:

$$\begin{cases} \alpha_1 = 0.5 \bullet \left[1 + \tanh\left(\dfrac{CS - x}{l}\right)\right] \\ \alpha_2 = 0.5 \bullet \left[1 + \tanh\left(\dfrac{x - \mathrm{CS}}{l}\right)\right] \end{cases} \quad (5)$$

At this crossover point, $\alpha_1 = \alpha_2 = \frac{1}{2}$. l is a scaling factor representing the rate or velocity of decrease or increase of a process [27]. Here α_1 represents the low degradative process, while α_2 denotes the high degradative one.

The evolution of the degradation processes is shown in Fig. 9 where the crossover point is at CS = 12%. At this point both processes contribute with 50% to the total degradation. In order to obtain reliable lifetime predictions for the given EPDM using CS after tempering, it is better to start when all samples at the different test temperatures have reached CS = 12% where the two processes (low and high) are activated. In Fig. 7, such CS value is reached after 1093 d (≈3 a) for the ageing temperature of 75 °C. This also explains why different slopes in the Arrhenius diagram were found [13] even after 2 a of ageing.

3.3. Influence of ageing on the leak-tightness during dynamic partial release

In the following, a method is presented that enables lifetime predictions based on the recovery ability of a seal. Leakage rate or similar tightness measurements are the only direct method for assessing the sealing function and thus the most important performance criterion of the seal during service. The gas leakage in elastomer seals arises both from gas permeation through the material and from the interfacial leakage through (micro) gaps between flange and seal [28] or due to the loss of contact [29]. Leakage rate measurements were performed using the pressure-rise method [11] including a small fast partial release of the

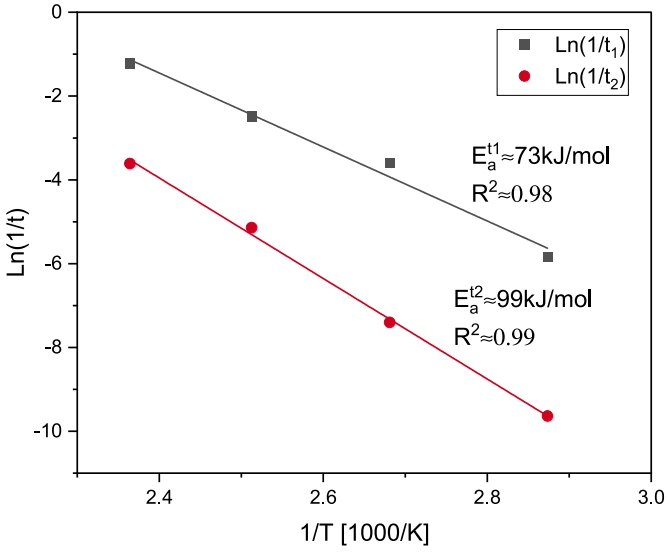

Fig. 8. Activation energies based on the retardation times of CS after tempering.

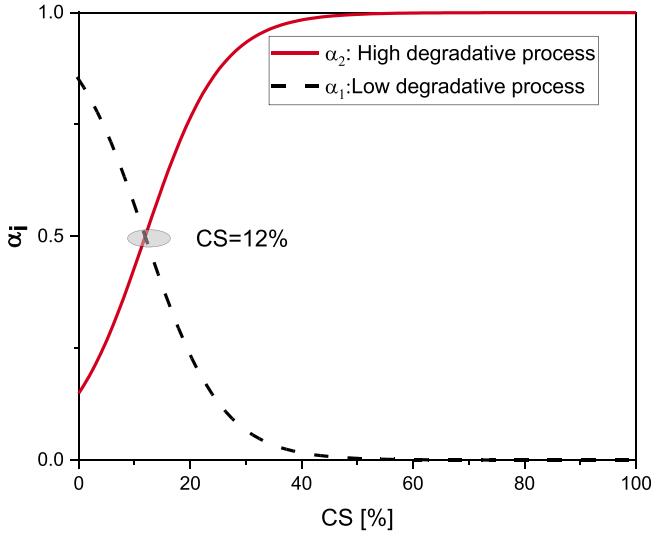

Fig. 9. Evolution of the degradative processes by means of CS.

seal from 25% to 23% compression in 1 s [12,15]. Contrary to most static leak-tightness investigations made on elastomer O-rings [30], this approach takes into account a safety margin for small dynamic events under accident scenarios. Thus, this test requires a certain amount of fast short-term recovery from the seal. To understand the influence of ageing on the leak-tightness during dynamic partial release, it is important to analyse the thermomechanical history of the seal and its effect on the restoring force. The elastomer O-ring was first mounted between flanges and compressed by 25%. Then, the flanges with the compressed O-ring were placed at elevated temperature for a given ageing time. In a compressed state at elevated temperature, the elastomer is forced to configurational changes causing the molecular chains to slide and stretch [31]. The elastomer is in a "constrained" state. During this state, physical and chemical changes occur in the network structure, such as compression stress relaxation, chain scission and formation of new crosslinks [32]. However, the newly formed crosslinks do not contribute to the stress relaxation [33,34]. After the ageing time has elapsed, the compressed O-ring between flanges was removed from the oven and allowed to cool down to RT. The elastomer undergoes thermal contractions upon cooling [16]. Still in compressed state, the elastomer is again in an intermediate state of equilibrium until load removal. After cooling, the flange system and the O-ring are mounted in the leakage rate apparatus. In static condition, where permeation leakage is likely most important, it has been found that both permeation and interfacial leakages are significant [28]. In the dynamic condition, the main cause of leakage is the inability of the seal to follow the movement of the flange during fast decompression. The pressure rise measurements after fast decompression lasts 2 h. When a pronounced increase in pressure is observed, this means that a leak gap opened up. However, the leakage rate can reduce again during the 2 h, which can be due to slow recovery of the seal that closes the gap. The decreasing pressure difference between outside and inside of the seal also leads to a reduction of gas flow and thus leakage rate over time.

To determine the point of seal failure associated with a notable leakage rate increase (usually by several orders of magnitude), an analysis of the CS is proposed. The shift factors of 150 °C–125 °C from different CS measurements are collected in Table 6. The same shift factor of 1/5 for CS measurements after 1 s that were performed with the DMA machine (Fig. 3) and CS after tempering [13] is found. Note that CS after tempering reflects the irreversible chemical processes while CS after 1 s and after 30 min include both physical and chemical processes. On the other hand, there are differences in CS values after 30 min measured with the DMA machine and those taken according to DIN ISO 815-1 from half O-rings compressed between plates as shown in Fig. 3. This means that for lifetime estimations based on dynamic fast partial release measurements, the CS data after tempering could be used as they have the same shift factor as those after 1 s. The corresponding ageing state can be linked to the respective CS value using the fit functions shown above, enabling to define a general CS-based end-of-lifetime criterion.

The leakage test with partial decompression has been performed on two rings aged at 150 °C and 125 °C, respectively. The results for the last ageing states of leak-tightness and the appearance of a significant pressure increase after the partial decompression as well as the corresponding CS values (after tempering, cf. Fig. 7) are shown in Table 7. At 150 °C, O-rings remained leak-tight for up to 70 d of ageing (86% CS) but became untight after 80 d (91% CS). For 125 °C, O-ring 1 was leak-tight up to 278 d (81% CS), but untight after 295 d (83% CS). However, after disassembly it was observed that the O-ring was not centered in the flange and thus slightly deformed on a spacer. Therefore, the results might not be representative. In the second experiment at 125 °C, the O-ring remained leak-tight for up to 300 d (83% CS) and was untight after 305 d (84% CS). Most of these data have been published before in Ref. [13]. New here are the results for the second O-ring at 125 °C and the more exact determination of the corresponding CS values by using the fit functions from Fig. 7. Conservatively, the last point of leak-tightness of the improperly assembled first 125 °C O-ring was chosen as the point defining the end-of-lifetime. Thus, an end-of-lifetime criterion of 80% CS (after tempering) for static seals including a safety margin for small dynamic events could be specified.

Table 6
Shift factors of different CS measurements.

	CS-30min	CS-Temp	CS-DMA-1s
Shift factors a_T 150 °C → 125 °C	1/4	1/5	1/5

Table 7
O-ring leak-tightness results.

	150 °C		125 °C	
	Leak-tight	Untight	Leak-tight	Untight
O-ring 1	70 d/86% CS[a]	100 d/94% CS	278 d/81% CS[a]	295 d/83% CS[a]
O-ring 2	70 d/86% CS[a]	80 d/91% CS	300 d/83% CS[a]	305 d/84% CS[a]

[a] Values determined with the fit functions of Fig. 7.

Using the fit functions from Fig. 7 and Table 5, this criterion would be reached after 7 a and 65 a for EPDM aged at 100 °C and 75 °C, respectively. However, the shift factor of 150 °C–125 °C from the leak-tightness results that are shown in Table 7 is 1/4. The difference between the shift factors based on the leak-tightness (1/4, from Table 7) and the CS measurements after tempering and after 1 s (1/5, see Table 6) can result from several error factors. Note that in our CS measurements there is an error of ±3%. Even though the correlation coefficients of the interpolation functions are close to 1, the manual shift of the data can present uncertainties. Besides, an error due to the interpolation function (Fig. 7) must be considered. As CS measurements after 30 min taken with the DMA device as well as the results according to DIN ISO 815-1 [8] standard are different (see Fig. 3), they are excluded from the comparison of the shift factors (Tables 6 and 7) although they are coincidentally the same (1/4). The difference in shift according to the criterion (leak-tightness or CS) has no influence on the fact that the end-of-lifetime criterion of 80% CS after tempering can be assumed as a conservative end-of-lifetime criterion.

4. Conclusion

For the EPDM material of the present study and the ageing temperatures 75 °C, 100 °C, 125 °C and 150 °C, it has been shown that:

- The short-term physical recovery is more pronounced for less degraded samples.
- The long-term physical recovery is faster for the more degraded samples compared to the less aged ones up to about 50 d after disassembly.
- Measuring CS after tempering enables to assess only the irreversible processes, which would otherwise be reached after about one year at room temperature for samples aged at 125 °C.
- For samples aged at 150 °C, the recovery almost comes to an end after about 50 d. However, the CS value after tempering is still lower.
- The drop of the CS of EPDM aged at 125 °C and 150 °C for 10 d within the first 20 d after disassembly is more pronounced for the more degraded sample.
- For lifetime predictions based on CS after tempering it is important to make the lifetime estimations after reaching CS = 12% for the material of the present study and the given ageing temperatures as the high degradation process that limits the lifetime becomes dominant at this point.
- The same shift factor between 150 °C and 125 °C was obtained for CS after 1 s and CS after tempering. Therefore, tentative lifetime predictions for the lower temperatures could be made for the fast decompression experiments.
- 80% CS after additional tempering could be set as a conservative leak-tightness criterion for the given EPDM, configuration and test

set-up for static seals including a safety margin for small dynamic events.

The obtained results will serve to improve the existing material model used in the simulation of interfacial leakage [35].

Author statement

M.Z, A.K., M.J. and D.W. designed the experiments; M.Z, A.K. and M. J. performed the experiments; M.Z., A.K., M.J. and D.W. analysed the data; M.Z. prepared the original draft; M.Z, A.K., M.J. and D.W. reviewed the manuscript.

Declaration of competing interest

The authors declare that they have no known competing financial interests or personal relationships that could have appeared to influence the work reported in this paper.

Data availability

Data will be made available on request.

Acknowledgements

Parts of this research were funded by The German Federal Ministry of Economic Affairs and Energy (BMWi, Project No. 1501509) on the basis of a decision by the German Bundestag.

References

[1] G.W. Ehrenstein, S. Pongratz, Beständigkeit von Kunststoffen, Carl Hanser, München, 2007.
[2] C. Li, Y. Ding, Z. Yang, Z. Yuan, L. Ye, Compressive stress-thermo oxidative ageing behaviour and mechanism of EPDM rubber gaskets for sealing resilience assessment, Polym. Test. 84 (2020), 106366, https://doi.org/10.1016/j.polymertesting.2020.106366.
[3] ISO 188, Rubber, Vulcanized or Thermoplastic—Accelerated Ageing and Heat Resistance Tests, 2011.
[4] A. Kömmling, M. Jaunich, D. Wolff, Effects of heterogeneous aging in compressed HNBR and EPDM O-ring seals, Polym. Degrad. Stabil. 126 (2016) 39–46, https://doi.org/10.1016/j.polymdegradstab.2016.01.012.
[5] A.I. Isayev, D. Cao, B. Dinzburg, Elastic recovery of rubber vulcanizates at very short times, J. Elastomers Plastics 28 (1996) 344–381, https://doi.org/10.1177/009524439602800406.
[6] M. Zaghdoudi, A. Kömmling, M. Jaunich, D. Wolff, Scission, cross-linking, and physical relaxation during thermal degradation of elastomers, Polymers 11 (2019) 1280, https://doi.org/10.3390/polym11081280.
[7] ASTM D395-18, Standard Test Methods for Rubber Property—Compression Set, ASTM International, West Conshohocken, PA, 2018. www.astm.org.
[8] DIN ISO 815-1:2019, Rubber, Vulcanized or Thermoplastic – Determination of Compression Set – Part 1: at Ambient or Elevated Temperatures, Beuth publisher, 2019. D, www.beuth.de.
[9] D. Wolff, H. Völzke, A. Bevilacqua, C. Alejano, J.M. Conde, R.E. Einziger, S. I. Fukuda, A. González Espartero, S. Gouzy-Portaix, R.E. Haddad Andalaf, D. Hambley, H. Issard, J. Kessler, L. Kurpaska, A. Legat, A.H. Qureshi, J. Ruiz, K. Shirai, A. Šmaižys, C.A. Verrastro, Demonstrating performance of spent fuel and related storage system components during very long term storage - final report of a coordinated research project, in: A. González Espartero (Ed.), IAEA TecDoc Series, IAEA Publishing Section, Vienna, Austria, 2019, pp. 1–198. https://www.iaea.org/publications/13553/demonstrating-performance-of-spent-fuel-and-related-storage-system-components-during-very-long-term-storage.
[10] M. Zaghdoudi, A. Kömmling, M. Jaunich, D. Wolff, Erroneous or Arrhenius: a degradation rate-based model for EPDM during homogeneous ageing, Polymers 12 (2020) 2152, https://doi.org/10.3390/polym12092152.
[11] A. Kömmling, M. Jaunich, P. Pourmand, D. Wolff, U.W. Gedde, Influence of Ageing on Sealability of Elastomeric O-Rings, vol. 373, Macromolecular Symposia, 2017, 1600157, https://doi.org/10.1002/masy.201600157.
[12] A. Kömmling, M. Jaunich, P. Pourmand, D. Wolff, M. Hedenqvist, Analysis of O-ring seal failure under static conditions and determination of end-of-lifetime criterion, Polymers 11 (2019) 1251, https://doi.org/10.3390/polym11081251.
[13] A. Kömmling, M. Jaunich, M. Goral, D. Wolff, Insights for lifetime predictions of O-ring seals from five-year long-term aging tests, Polym. Degrad. Stabil. 179 (2020), 109278, https://doi.org/10.1016/j.polymdegradstab.2020.109278.
[14] K.T. Gillen, R. Bernstein, M.H. Wilson, Predicting and confirming the lifetime of o-rings, Polym. Degrad. Stabil. 87 (2005) 257–270, https://doi.org/10.1016/j.polymdegradstab.2004.07.019.
[15] T. Grelle, D. Wolff, M. Jaunich, Temperature-dependent leak tightness of elastomer seals after partial and rapid release of compression, Polym. Test. 48 (2015) 44–49, https://doi.org/10.1016/j.polymertesting.2015.09.009.
[16] R.E. Morris, J.W. Hollister, A.E. Barrett, Cold compression set of elastomer vulcanizates, Ind. Eng. Chem. 42 (1950) 1581–1587, https://doi.org/10.1021/ie50488a034.
[17] M. Zaghdoudi, A. Kömmling, M. Jaunich, D. Wolff, Oxidative ageing of elastomers: experiment and modelling, Continuum Mech. Therm. (2022), https://doi.org/10.1007/s00161-022-01093-9.
[18] R.A. Assink, K.T. Gillen, B. Sanderson, Monitoring the degradation of a thermally aged EPDM terpolymer by 1H NMR relaxation measurements of solvent swelled samples, Polymer 43 (2002) 1349–1355, https://doi.org/10.1016/S0032-3861(01)00661-9.
[19] A. Kumar, S. Commereuc, V. Verney, Ageing of elastomers: a molecular approach based on rheological characterization, Polym. Degrad. Stabil. 85 (2004) 751–757, https://doi.org/10.1016/j.polymdegradstab.2003.11.014.
[20] M.M. Rahman, V. Abetz, Tailoring crosslinked polyether networks for separation of CO2 from light gases, Macromol. Rapid Commun. 42 (2021), 2100160, https://doi.org/10.1002/marc.202100160.
[21] R. Bernstein, K.T. Gillen, Predicting the lifetime of fluorosilicone o-rings, Polym. Degrad. Stabil. 94 (2009) 2107–2113, https://doi.org/10.1016/j.polymdegradstab.2009.10.005.
[22] M. Celina, K. Gillen, M.R. Keenan, Methods for Predicting More Confident Lifetimes of Seals in Air Environments, Sandia National Lab.(SNL-NM), Albuquerque, NM (United States); Sandia, 1999.
[23] M. Celina, J. Wise, D.K. Ottesen, K.T. Gillen, R.L. Clough, Oxidation profiles of thermally aged nitrile rubber, Polym. Degrad. Stabil. 60 (1998) 493–504, https://doi.org/10.1016/S0141-3910(97)00113-4.
[24] K. Xiang, G. Huang, J. Zheng, X. Wang, J. Huang, Investigation on the thermal oxidative aging mechanism and lifetime prediction of butyl rubber, Macromol. Res. 21 (2013) 10–16, https://doi.org/10.1007/s13233-012-0174-3.
[25] M. Celina, K.T. Gillen, R.A. Assink, Accelerated aging and lifetime prediction: review of non-Arrhenius behaviour due to two competing processes, Polym. Degrad. Stabil. 90 (2005) 395–404, https://doi.org/10.1016/j.polymdegradstab.2005.05.004.
[26] K.T. Gillen, M. Celina, R.L. Clough, J. Wise, Extrapolation of accelerated aging data-Arrhenius or erroneous? Trends Polym. Sci. 8 (1997) 250–257.
[27] L.D. Roper, Depletion theory, Depletion Theory 1 (1976) 6.
[28] N.G. Garafolo, C.C. Daniels, An Empirical Investigation on Seal-Interface Leakage of an Elastomer Face Seal, ASME 2012 Fluids Engineering Division Summer Meeting Collocated with the ASME 2012 Heat Transfer Summer Conference and the ASME 2012 10th International Conference on Nanochannels, Microchannels, and Minichannels, 2012, pp. 969–979.
[29] A. Akulichev, A. Echtermeyer, B. Persson, Interfacial leakage of elastomer seals at low temperatures, Int. J. Pres. Ves. Pip. 160 (2018) 14–23, https://doi.org/10.1016/j.ijpvp.2017.11.014.
[30] S. Momon, J. Garcia, H. Issard, Leak tightness of O-rings for transport of radioactive material, Packag. Transp. Storage Secur. Radioact. Material 24 (2013) 3–9, https://doi.org/10.1179/1746510913Y.0000000033.
[31] J. Peters, V.v. Wollesen, O. von Estorff, M. Achenbach, On the modelling of the viscoelastic behaviour of elastomers based on irreversible thermodynamics, KGK. Kautschuk, Gummi, Kunststoffe 62 (2009) 98–102.
[32] W. Lou, W. Zhang, X. Liu, T. Lou, D. Xu, Effects of medium phases on the thermal degradation of hydrogenated nitrile rubber O-rings under compression, J. Appl. Polym. Sci. 135 (2018), 45864, https://doi.org/10.1002/app.45864.
[33] A.V. Tobolsky, I.B. Prettyman, J.H. Dillon, Stress relaxation of natural and synthetic rubber stocks, J. Appl. Phys. 15 (1944) 380–395, https://doi.org/10.1063/1.1707442.
[34] R.D. Andrews, A.V. Tobolsky, E.E. Hanson, The theory of permanent set at elevated temperatures in natural and synthetic rubber vulcanizates, J. Appl. Phys. 17 (1946) 352–361, https://doi.org/10.1063/1.1707724.
[35] M. Weber, M. Zaghdoudi, A. Kömmling, M. Jaunich, D. Wolff, A Numerical Approach to Correlate Compression Stress Relaxation and Compression Set of Elastomer O-Rings with Tightness, ASME 2021 Pressure Vessels & Piping Conference, 2021.